Semiclassical density of degeneracies in quantum regular systems

2000 J. Phys. A: Math. Gen. 33 2345

(http://iopscience.iop.org/0305-4470/33/12/303)

J. Phys. A: Math. Gen. **33** (2000) 2345–2363. Printed in the UK PII: S0305-4470(00)08436-5

Semiclassical density of degeneracies in quantum regular systems

A J Fendrik and M J Sánchez

Departamento de Física J J Giambiagi, Facultad de Ciencias Exactas y Naturales, Universidad de Buenos Aires, Ciudad Universitaria, 1428 Buenos Aires, Argentina

Received 5 October 1999

Abstract. The spectrum of eigenenergies of a quantum integrable system whose Hamiltonian depends on a single parameter shows degeneracies (crossings) when the parameter varies. We derive a semiclassical expression for the density of crossings in the plane energy–parameter, that is the number of crossings per unit of energy and unit of parameter, in terms of classical periodic orbits. We compare the results of the semiclassical formula with exact quantum calculations for two specific quantum integrable billiards.

Introduction

The analysis of energy spectra of different physical bounded systems has always been an interesting subject in quantum mechanics. The energy level spacings as well as the existence of degeneracies (crossings) in such systems have been widely studied during recent years. The number of degrees of freedom, the separability of the problem and the number of free parameters involved, among others, are very important features which have to be taken into account when a given quantum spectrum is analysed.

Starting from Percival's ideas [1] for systems with more than one degree of freedom, two kinds of spectra have been distinguished. The regular spectrum, whose level spacing is characterized by a Poisson distribution [2], is associated with integrable problems (the harmonic oscillator is an exception). The other one, the irregular spectrum closely characterized by spectral statistic of the Gaussian ensembles, corresponds to non-integrable systems [3–5]. This statistical behaviour can be related to crossings and repulsions between levels with the same symmetry when the spectra are analysed as a function of the parameters of the problem. In fact, integrable systems depending on one parameter exhibit many crossings while non-integrable systems show repulsions and double-hyperbola curves (avoided crossings), rather than degeneracies. So, for one-parameter-dependent systems, the presence of crossings or avoided crossings are quantum fingerprints of the properties of the classical dynamics. When the system depends on two parameters, the surfaces of energy (that define in such cases the eigenenergies) will cross in continuum curves leading to diedric intersections when the system remains integrable, or they will intersect at isolated points ('diabolical points') if the system is not integrable (assuming that it has time reversal symmetry) [6].

Distributions of avoided crossings (for one-parameter-dependent systems) according to properties such that the closest approach or the mean and difference between the slopes of the involved levels were already established for a generic quantum system employing parametric random-matrix models [7, 8]. The same models, extended to two and more parameters, were

0305-4470/00/122345+19$30.00

used to study distributions of diabolical points [9] and other relevant distributions of singular points in the spectra [10].

On the other hand, it is well known that classical periodic orbits are essential elements to develop semiclassical quantization methods. Not only for integrable systems (through the Berry–Tabor formula [11]) but also for the non-integrable ones (using the Gutzwiller methods [12]), the spectral density can be formally described in terms of closed orbits of the classical system. Therefore, it would not be surprising that other quantum densities such as densities of degeneracies or densities of avoided crossings can be related to the periodic orbits.

In this paper, we find the density of degeneracies as an expansion in terms of the periodic orbits for classical integrable systems depending on one parameter.

In section 1 we introduce the density of degeneracies. The semiclassical version can be written as a sum of a smooth part and oscillating contributions depending on the periodic orbits of the classical system. Section 2 is devoted to compute the smooth part of the density of degeneracies and related distributions for two specific integrable systems whose Hamiltonians depend on a single parameter in a different functional form. We study the rectangular billiard of sides a and b where the parameter is the ratio $\mu = b/a$ (shape parameter) and the Aharonov–Bohm cylindrical billiard where the parameter is the magnetic flux, that is $\mu = \phi$. The oscillating contributions are computed in section 3. Finally, section 4 is devoted to concluding remarks. We have included an appendix that contains the appropriate derivations of the semiclassical density of degeneracies when conjugated states by time reversal transformation could be not degenerated (like the Aharonov–Bohm cylindrical billiard).

1. The density of degeneracies

We consider an integrable system whose Hamiltonian depends on a single parameter μ. That is

$$H = H(\vec{I}, \mu) \tag{1.1}$$

where $\vec{I} \equiv (I_1, \ldots, I_n)$ and $I_i = \frac{1}{2\pi} \oint p_i \, \mathrm{d}q_i$ are the action variables. To obtain the eigenvalues, we can employ the EBK semiclassical quantization rule

$$I_i = \hbar \left(n_i + \frac{\alpha_i}{4} \right) \tag{1.2}$$

where $n_i = 0, 1, 2, \ldots$ and α_i are the Maslov index [12]. So, we establish the quantum eigenenergies E by

$$E(\vec{n}, \mu) = H\left(\vec{n} + \frac{\vec{\alpha}}{4}, \mu \right). \tag{1.3}$$

When we consider the eigenenergies as a function of the parameter μ, the spectrum shows degeneracies (crossings). They occur whenever

$$H\left(\vec{n} + \frac{\vec{\alpha}}{4}, \mu \right) - H\left(\vec{n}' + \frac{\vec{\alpha}}{4}, \mu \right) = 0. \tag{1.4}$$

Given $\vec{n}$ and $\vec{n}'$, this equation determines the values of the parameter μ for which the eigenenergies labelled by $\vec{n}$ and $\vec{n}'$ are degenerated,

$$\mu = L\left(\vec{n} + \frac{\vec{\alpha}}{4}, \vec{n}' + \frac{\vec{\alpha}}{4} \right). \tag{1.5}$$

We define the density of degeneracies $\rho_c(E, \mu)$ as the number of crossings that occurs in the energy interval $[E, E + \mathrm{d}E]$ and in the parameter interval $[\mu, \mu + \mathrm{d}\mu]$.

Therefore, using the EBK rule, we can write $\rho_c(E,\mu)$ as follows:

$$\rho_c(E,\mu)=\frac{1}{2}\sum_{\vec{n}}\sum_{\vec{n}'}\delta\left(E-H\left(\vec{n}+\frac{\vec{\alpha}}{4},\mu\right)\right)\delta\left(\mu-L\left(\vec{n}+\frac{\vec{\alpha}}{4},\vec{n}'+\frac{\vec{\alpha}}{4}\right)\right) \tag{1.6}$$

where we disregard as in [2] possible degeneracy factors. The diagonal terms in equation (1.6) deserve some comments (see appendix A). Employing the Poisson summation formula in equation (1.6) we write

$$\begin{aligned}\rho_c(E,\mu)=&\frac{1}{2\hbar^{2n}}\sum_{\vec{m}}\sum_{\vec{m}'}\exp\left[-\mathrm{i}\frac{\pi}{2}(\vec{\alpha}\cdot\vec{m}+\vec{\alpha}\cdot\vec{m}')\right]\\&\times\int_{\vec{I}\geqslant 0}\int_{\vec{I}'\geqslant 0}\mathrm{d}^nI\,\mathrm{d}^nI'\delta(E-H(\vec{I},\mu))\delta(\mu-L(\vec{I},\vec{I}'))\\&\times\exp\left[\mathrm{i}\frac{2\pi}{\hbar}(\vec{m}\cdot\vec{I}+\vec{m}'\cdot\vec{I}')\right].\end{aligned} \tag{1.7}$$

In the following, to make the expressions more easily handled, we assume two degrees of freedom.

To eliminate the δ-functions, we change the integration variables as follows:

$$(I_1,I_1',I_2,I_2')\to(I_1,I_1',\xi_1,\xi_2) \tag{1.8}$$

where we have defined

$$\begin{aligned}\xi_1&\equiv E-H(I_1,I_2,\mu)\\\xi_2&\equiv\mu-L(I_1,I_2,I_1',I_2').\end{aligned} \tag{1.9}$$

Therefore

$$\mathrm{d}I_1\,\mathrm{d}I_2\,\mathrm{d}I_1'\,\mathrm{d}I_2'=\frac{1}{|\frac{\partial H}{\partial I_2}\frac{\partial L}{\partial I_2'}|}\mathrm{d}I_1\,\mathrm{d}I_2\,\mathrm{d}\xi_1\,\mathrm{d}\xi_2. \tag{1.10}$$

The partial derivative $\partial L/\partial I_2'$ is defined by the implicit equation

$$H(I_1,I_2,L)-H(I_1',I_2',L)=0 \tag{1.11}$$

and we obtain

$$\left|\frac{\partial L}{\partial I_2'}\right|=\frac{1}{|\frac{\partial H}{\partial L})_I-\frac{\partial H}{\partial L})_{I'}|}\frac{\partial H}{\partial I_2'} \tag{1.12}$$

where $\frac{\partial H}{\partial L})_I$ and $\frac{\partial H}{\partial L})_{I'}$ are the partial derivatives evaluated in I and I'. After integration over ξ_1 and ξ_2 follows

$$\begin{aligned}\rho_c(E,\mu)=&\frac{1}{2\hbar^4}\sum_{\vec{m}}\sum_{\vec{m}'}\exp\left[-\mathrm{i}\frac{\pi}{2}(\vec{\alpha}\cdot\vec{m}+\vec{\alpha}\cdot\vec{m}')\right]\\&\times\int_{I_1\geqslant 0}\int_{I_1'\geqslant 0}\mathrm{d}I_1\,\mathrm{d}I_1'\frac{|\partial_\mu H-\partial_\mu H'|}{\omega_2\omega_2'}\exp\left[\mathrm{i}\frac{2\pi}{\hbar}(\vec{m}\cdot\vec{I}+\vec{m}'\cdot\vec{I}')\right]\end{aligned} \tag{1.13}$$

where

$$\partial_\mu H\equiv\frac{\partial H(I_1,I_2(E,I_1),\mu)}{\partial\mu} \tag{1.14}$$

$$\partial_\mu H'\equiv\frac{\partial H(I_1',I_2'(E,I_1'),\mu)}{\partial\mu} \tag{1.15}$$

$$\omega_2\equiv\frac{\partial H(I_1,I_2,\mu)}{\partial I_2} \tag{1.16}$$

$$\omega_2'\equiv\frac{\partial H(I_1',I_2',\mu)}{\partial I_2'}. \tag{1.17}$$

The first term in equation (1.13) (with $m_1 = m_2 = m_1' = m_2' = 0$) corresponds to replacing the quadruple sum in equation (1.6) by the quadruple integral. It is a smooth function (i.e. non-oscillating) of E and μ,

$$\langle \rho_c(E, \mu) \rangle = \frac{1}{2\overline{h}^4} \int_{I_1} \int_{I_1'} \mathrm{d}I_1 \, \mathrm{d}I_1' \frac{|\partial_\mu H - \partial_\mu H'|}{\omega_2 \omega_2{}'}. \tag{1.18}$$

Starting from equation (1.18) we can determine other relevant distributions. As an example, we can obtain the smooth part of the distribution of crossings $\langle \rho_c(E, \mu, V) \rangle$ according to the difference between the slopes of the levels,

$$V \equiv |\partial_\mu H - \partial_\mu H'|. \tag{1.19}$$

To obtain such a distribution (in the following DCDS), we perform the change of the integration variables in equation (1.18)

$$(I_1, I_1') \to (I_1, V). \tag{1.20}$$

Therefore

$$\mathrm{d}I_1 \, \mathrm{d}I_1' = \frac{\mathrm{d}I_1 \, \mathrm{d}V}{|\partial_\mu \omega_1' - (\frac{\omega_1'}{\omega_2'}) \partial_\mu \omega_2'|} \tag{1.21}$$

where the ω must be considered as a function of I_1, V and μ. Leaving out the integration over V, follows

$$\langle \rho_c(E, \mu, V) \rangle = \frac{1}{2\overline{h}^4} V \int_{I_1} \frac{\mathrm{d}I_1}{\omega_2 |\omega_2' \partial_\mu \omega_1' - \omega_1' \partial_\mu \omega_2'|}. \tag{1.22}$$

We stress that the dependence on V in equation (1.22) is not only given by the prefactor V but also by the integrand and the limits of integration in the integral over I_1.

The other terms in equation (1.13) contain oscillating functions and we utilize the stationary phase technique to evaluate them. The conditions of stationary phase lead to the periodicity conditions, namely

$$\frac{\omega_1}{\omega_2} = \frac{m_1}{m_2} \tag{1.23}$$

$$\frac{\omega_1'}{\omega_2'} = \frac{m_1'}{m_2'}. \tag{1.24}$$

Because ω_k (ω_k') are positive, the sums over m_k (m_k') in equation (1.13) are restricted to the first and the third quadrants. The numbers m_1, m_2 define the topology of the periodic orbits. However, there could be pairs of periodic orbits that having the same topology, they are related to each other through time reversal transformation (non-self-retracing orbits).

For the terms $m_1 \neq 0, m_2 \neq 0, m_1' = m_2' = 0$ ($m_1 = m_2 = 0, m_1' \neq 0, m_2' \neq 0$) we first perform the integration over the variable $I_1'(I_1)$ and next we evaluate the second integral using the stationary phase approximation. Finally, we obtain

$$\rho_c(E, \mu)_{osc1} = \frac{1}{\overline{h}^{7/2}} \sum_{m_1, m_2 \neq (0,0)} \frac{\Delta_{m_1, m_2}}{|m_2 \frac{\mathrm{d}^2 I_2}{\mathrm{d}I_1^2}|^{1/2}} \left[\int_{I_1' \geqslant 0} P(I_1^o, I_1') \, \mathrm{d}I_1' \right] \times \cos\left(S(m_1, m_2)/\overline{h} + \theta(m_1, m_2)\right) \tag{1.25}$$

where we have defined

$$P(X, Y) \equiv \left| \frac{\partial_\mu H(X) - \partial_\mu H'(Y)}{\omega_2(X) \omega_2(Y)} \right| \tag{1.26}$$

$$S(m_1, m_2) \equiv 2\pi (m_1 I_1^o + m_2 I_2^o) \tag{1.27}$$

$$\theta(m_1, m_2) \equiv \frac{\pi}{4}\mathrm{sig}\left(m_2 \frac{\mathrm{d}^2 I_2}{\mathrm{d}I_1^2}\right) - \frac{\pi}{2}(\alpha_1 m_1 + \alpha_2 m_2) \tag{1.28}$$

$$\Delta_{m_1,m_2} \equiv \begin{cases} 2 & \text{if there are two orbits of topology } m_1, m_2 \\ 1 & \text{otherwise.} \end{cases} \tag{1.29}$$

$I_1^o = I_1^o(m_1, m_2)$, $I_2^o = I_2^o(m_1, m_2)$ are the values of the actions given by equation (1.23). On the other hand, for $m_1 \neq 0$ or $m_2 \neq 0$ and $m_1' \neq 0$ or $m_2' \neq 0$ we obtain

$$\rho_c(E, \mu)_{osc2} = \frac{2}{\hbar^3} \sum_{m_1, m_2 \neq (0,0)} \sum_{m_1', m_2' \neq (0,0)} \frac{\Delta_{m_1,m_2}\Delta_{m_1',m_2'} P(I_1^o(m_1, m_2), I_1'^o(m_1', m_2'))}{|m_2 m_2' \frac{\mathrm{d}^2 I_2}{\mathrm{d}I_1^2} \frac{\mathrm{d}^2 I_2'}{\mathrm{d}I_1'^2}|^{1/2}}$$
$$\times \cos\left(S(m_1, m_2)/\hbar + \theta(m_1, m_2)\right) \cos\left(S(m_1', m_2')/\hbar + \theta'(m_1', m_2')\right). \tag{1.30}$$

Let us remark that the summations over m_1, m_2 in equation (1.25) and over m_1, m_2, m_1', m_2' in equation (1.30) are restricted to the first quadrant.

2. The smooth part of the density of crossings

In this section we compute the smooth part of the density of crossing starting from equation (1.18) for two specific systems. We will consider two kinds of billiards whose Hamiltonian depend on the parameter μ in a different way.

2.1. Rectangular billiards

At first we study the well known rectangular billiard. That is a spinless particle in a two-dimensional rectangular box of sides a and b. The Hamiltonian in terms of the action variables is

$$H(I_1, I_2) = \frac{\pi^2}{2m}\left(\frac{I_1^2}{a^2} + \frac{I_2^2}{b^2}\right). \tag{2.1}$$

In this case we will consider the crossings as a function of the shape parameter $\mu = b/a$. We fix the area of the box $A = ab$ as a constant to conserve invariant the smooth part of the density of states. So the Hamiltonian can be written as

$$h = \mu I_1^2 + \frac{I_2^2}{\mu} \tag{2.2}$$

where $h \equiv \frac{2mAH}{\pi^2}$. In the following we will use the Hamiltonian given by equation (2.2) and we call the corresponding energy as $\epsilon \equiv \frac{2mAE}{\pi^2}$.

Taking into account that

$$I_2 = \sqrt{\mu\epsilon - \mu^2 I_1^2} \tag{2.3}$$

$$\omega_2 = \frac{2I_2}{\mu} \tag{2.4}$$

$$|\partial_\mu h - \partial_\mu h'| = 2|I_1^2 - I_1'^2| \tag{2.5}$$

and setting $\hbar = 1$, we obtain, after replacing in equation (1.18),

$$\langle \rho_c(\epsilon, \mu)\rangle = \frac{\mu}{4}\int_{I_1'=0}^{I_1'=\sqrt{\epsilon/\mu}} \frac{\mathrm{d}I_1'}{\sqrt{\epsilon - \mu I_1'^2}}\left[\int_{I_1=I_1'}^{I_1=\sqrt{\epsilon/\mu}} \frac{(I_1^2 - I_1'^2)\,\mathrm{d}I_1}{\sqrt{\epsilon - \mu I_1^2}} + \int_{I_1=0}^{I_1=I_1'} \frac{(I_1'^2 - I_1^2)\,\mathrm{d}I_1}{\sqrt{\epsilon - \mu I_1^2}}\right] \tag{2.6}$$

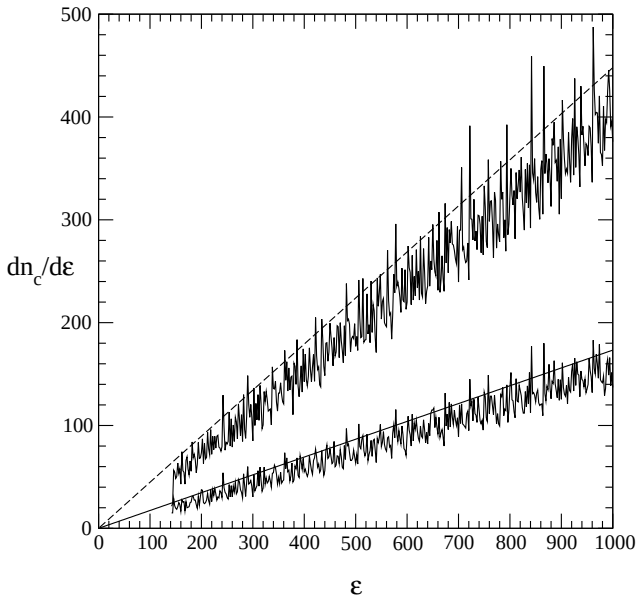

Figure 1. Integrated density of crossings $\frac{dn_c}{d\epsilon}$ as a function of the energy ϵ for the rectangular billiard. The straight lines correspond to the smooth part $\langle \frac{dn_c}{d\epsilon} \rangle = \frac{\epsilon}{4} \ln(\frac{\mu_2}{\mu_1})$ for $\mu_2 = 6$ (dashed line) and $\mu_2 = 2$ (solid line). In both cases $\mu_1 = 1$.

which after elementary integration leads to

$$\langle \rho_c(\epsilon, \mu) \rangle = \frac{1}{4} \frac{\epsilon}{\mu}. \tag{2.7}$$

To compare this result with the exact one obtained by quantum calculation, we integrate the above density of crossings over the parameter μ. In this way we establish the mean number of crossing in the finite interval $[\mu_1, \mu_2]$ with energies between ϵ and $\epsilon + d\epsilon$:

$$\begin{aligned} \left\langle \frac{dn_c}{d\epsilon}(\epsilon, \mu_1, \mu_2) \right\rangle &= \int_{\mu_1}^{\mu_2} \langle \rho_c(\epsilon, \mu) \rangle \, d\mu \\ &= \frac{1}{4} \epsilon \ln \left(\frac{\mu_2}{\mu_1} \right) \end{aligned} \tag{2.8}$$

which is a linear function of ϵ. Figure 1 shows the predictions of the preceding result for $\mu_1 = 1$ and $\mu_2 = 2$ (solid curve) and $\mu_2 = 6$ (dashed curve) together with the exact calculations.

Now we apply equation (1.22) to obtain the DCDS. We define the relative difference of slopes as $v \equiv V/V_{\max}$ where $V = 2|I_1^2 - I_2^2|$ and $V_{\max}$ is the highest value of V for a given value of the energy ϵ and the parameter μ (in the present example $V_{\max} = 2\epsilon/\mu$). By changing the variables in equation (2.6) $(I_1, I_1') \to (z = I_1\sqrt{\mu/\epsilon}, v)$ and leaving out the integration over v, we obtain

$$\langle \rho_c(\epsilon, \mu, v) \rangle = \frac{1}{4} \frac{\epsilon}{\mu} g(v) \tag{2.9}$$

where

$$g(v) = v \int_{z=\sqrt{v}}^{z=1} \frac{dz}{\sqrt{(1 - z^2)(1 - (z^2 - v))(z^2 - v)}}. \tag{2.10}$$

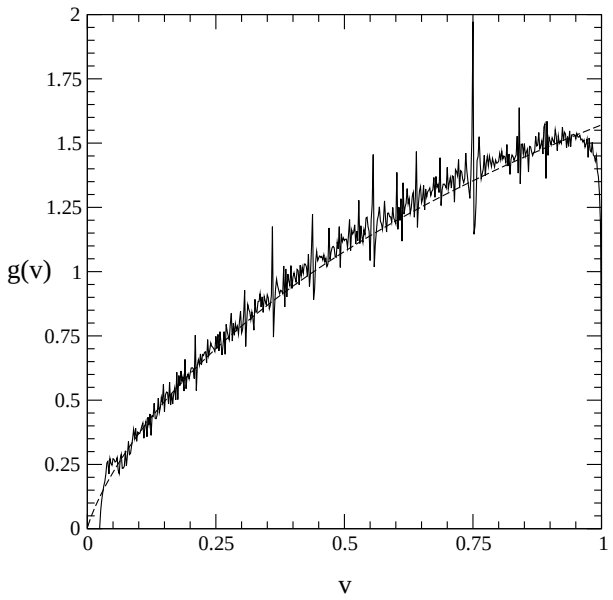

Figure 2. Distribution of crossings $g(v)$ according to the relative difference between the slopes v for the rectangular billiard. The result predicted for the smooth part of density of crossings corresponds to the dashed curve.

Therefore, the joint distribution equation (2.9) is factorizable as $\langle \rho_c(\epsilon, \mu) \rangle g(v)$. This means that the distribution of crossings according to the relative difference between the slopes of the levels is a global property of the system. It holds for any region in the plane ϵ–μ. Equation (2.10) is normalized to one and gives the fraction of crossings whose relative difference of slopes is in the interval $[v, v + \mathrm{d}v]$, and it is independent of the values of ϵ and μ. For example, the distribution of the number of crossings in the intervals $[0, \epsilon]$ and $[1, \mu]$ according to the difference of the slopes is

$$\left\langle \frac{\mathrm{d}n_c}{\mathrm{d}v} \right\rangle = \frac{\epsilon^2 \ln \mu}{8} g(v). \tag{2.11}$$

That is, if we construct a histogram of the relative difference between the slopes for all the crossings in the intervals $[0, \epsilon]$ and $[1, \mu]$, the smooth part of such a histogram will be given by equation (2.10). Figure 2 shows the distribution equation (2.10) together with the histogram resulting from the exact quantum calculation computing the relative difference between the slopes of the crossings that occur in the region $\epsilon < 3000$ and $1 \leqslant \mu \leqslant 2$ ($\sim$720 000 crossings).

2.2. Aharonov–Bohm cylindrical billiards

As a second example, we consider the Aharonov–Bohm cylindrical billiard. That is a spinless particle confined in a two-dimensional cylindrical shell of height a and radius r axially threaded by a confined magnetic flux ϕ. The Hamiltonian is (taking I_1 as non-negative)

$$H(I_1, I_2) = \frac{(I_1 \pm \frac{q\Phi}{2\pi c})^2}{2mr^2} + \frac{\pi^2 I_2^2}{2ma^2} \tag{2.12}$$

which can be rewritten as

$$h = \gamma (I_1 \pm \phi)^2 + I_2^2 \tag{2.13}$$

where $\gamma \equiv \frac{a^2}{\pi^2 r^2}$, $\phi \equiv \frac{q\Phi}{2\pi c}$ and $h \equiv \frac{2ma^2 H}{\pi^2}$. As in the first example we define the energy $\epsilon \equiv \frac{2ma^2 E}{\pi^2}$. Now, we will consider the crossings as a function of the normalized magnetic flux ϕ. That is we set $\mu = \phi$. Taking into account that

$$I_2 = \sqrt{\epsilon - \gamma(I_1 \pm \mu)^2} \tag{2.14}$$

$$\omega_2 = 2I_2 \tag{2.15}$$

$$|\partial_\mu h - \partial_\mu h'| = 2\gamma |I_1 \pm I_1'| \tag{2.16}$$

and setting $\overline{h} = 1$, we obtain

$$\langle \rho_c(\epsilon, \mu) \rangle = \gamma \int_{I_1'=0}^{I_1'=\sqrt{\epsilon/\gamma}} \frac{\mathrm{d}I_1'}{\sqrt{\epsilon - \gamma I_1'^2}} \left[\int_{I_1=I_1'}^{I_1=\sqrt{\epsilon/\gamma}} \frac{(I_1 - I_1')\,\mathrm{d}I_1}{2\sqrt{\epsilon - \gamma I_1^2}} + \int_{I_1=0}^{I_1=I_1'} \frac{(I_1' - I_1)\,\mathrm{d}I_1}{2\sqrt{\epsilon - \gamma I_1^2}} + \int_{I_1=0}^{I_1=\sqrt{\epsilon/\gamma}} \frac{(I_1 + I_1')\,\mathrm{d}I_1}{2\sqrt{\epsilon - \gamma I_1^2}} \right]. \tag{2.17}$$

To derive equation (2.17) it is necessary to take into account in equation (1.6) the effect of the breaking of the time reversal invariance (see appendix). After performing the integrations, equation (2.17) gives

$$\langle \rho_c(\epsilon, \mu) \rangle = \frac{2\sqrt{\epsilon}}{\sqrt{\gamma}}. \tag{2.18}$$

This smooth density of crossings is independent on the parameter μ (the flux). Therefore, the number of crossing between ϵ and $\epsilon + \mathrm{d}\epsilon$ per unit of flux is given by equation (2.18). Figure 3 shows $\langle \rho_c(\epsilon, \mu) \rangle$ given by equation (2.18) and the exact quantum calculation for a system with $\gamma = \frac{4}{\pi^2}$.

Starting from equation (2.17), it is not difficult to establish the DCDS. Let us distinguish the crossings according to the relative sign between the slopes. We label by a plus sign (+) (minus sign, (−)) the crossings between levels with equal (different) sign of their slopes. We can discriminate in equation (2.17) the contributions from both kinds of crossing. The first and second integral in the square bracket correspond to crossings with the same sign of the slopes while the third integral corresponds to crossings with different sign. Thus we find

$$\begin{aligned} \langle \rho_c(\epsilon, \mu) \rangle &= \langle \rho_c(\epsilon, \mu)^+ \rangle + \langle \rho_c(\epsilon, \mu)^- \rangle \\ \langle \rho_c(\epsilon, \mu)^+ \rangle &= \sqrt{\frac{\epsilon}{\gamma}} \left(2 - \frac{\pi}{2}\right) \\ \langle \rho_c(\epsilon, \mu)^- \rangle &= \sqrt{\frac{\epsilon}{\gamma}} \frac{\pi}{2}. \end{aligned} \tag{2.19}$$

Although the smooth part of the density of crossings depends on the energy ϵ and on the shape parameter γ, the fractions of each kind of crossing are the same for all cylinders and they are independent on the energies.

To establish the DCDS we proceed as follows. We define the relative jump of the slopes as

$$v = \sqrt{\frac{\gamma}{\epsilon}} |I_1 - I_1'| \tag{2.20}$$

for crossings with same sign of the slopes and

$$v = \sqrt{\frac{\gamma}{\epsilon}} (I_1 + I_1') \tag{2.21}$$

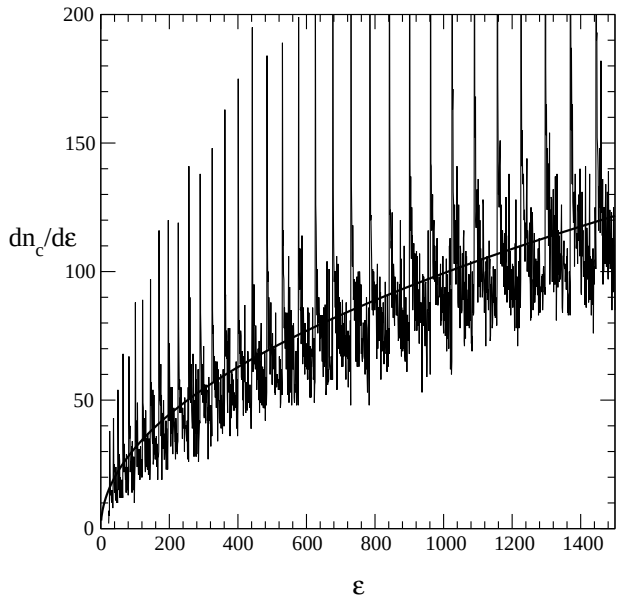

Figure 3. Integrated density of crossings $\frac{\mathrm{d}n_c}{\mathrm{d}\epsilon}$ as a function of energy ϵ for the Aharonov–Bohm cylindrical billiard with $\gamma = \frac{4}{\pi^2}$. The solid smooth curve corresponds to the smooth part $\langle \frac{\mathrm{d}n_c}{\mathrm{d}\epsilon} \rangle = 2\sqrt{\frac{\epsilon}{\gamma}}$.

for crossings with different slope signs. In this way v results $0 \leqslant v \leqslant 1$ for crossings labelled (+) while it is $0 \leqslant v \leqslant 2$ for crossings (−).

Thus, by changing variables in equation (2.17) and leaving out the integration over v we obtain

$$\langle \rho_c(\epsilon, \mu, v) \rangle = \begin{cases} 2\sqrt{\dfrac{\epsilon}{\gamma}}(g_I(v)^+ + g_I(v)^-) & \text{if} \quad v \leqslant 1 \\ 2\sqrt{\dfrac{\epsilon}{\gamma}} g_{II}(v)^- & \text{if} \quad 2 \geqslant v > 1 \end{cases} \tag{2.22}$$

where

$$\begin{aligned} g_I(v)^+ &= \frac{1}{2} v \int_v^1 \frac{\mathrm{d}z}{\sqrt{1-(z-v)^2}\sqrt{1-z^2}} \\ g_I(v)^- &= \frac{1}{4} v \int_0^v \frac{\mathrm{d}z}{\sqrt{1-(v-z)^2}\sqrt{1-z^2}} \\ g_{II}(v)^- &= \frac{1}{4} v \int_{v-1}^1 \frac{\mathrm{d}z}{\sqrt{1-(v-z)^2}\sqrt{1-z^2}}. \end{aligned} \tag{2.23}$$

Equation (2.22) gives the mean number of crossings per unit of flux that occur in the interval of energy $[\epsilon, \epsilon + \mathrm{d}\epsilon]$ and such that the relative difference between the slopes lies in the interval $[v, v+\mathrm{d}v]$ per unit of flux. For $v \leqslant 1$ there are two contributions. The first integral corresponds to crossings with the same slope signs and the second one corresponds to crossings between levels with different slope signs. For $v > 1$, only crossings with different slope signs can occur. Let us remark that the joint distribution $\langle \rho_c(\epsilon, \mu, v) \rangle$ is factorizable (as in the rectangular billiard)

$$\langle \rho_c(\epsilon, \mu, v) \rangle = \langle \rho_c(\epsilon, \mu) \rangle g(v) \tag{2.24}$$

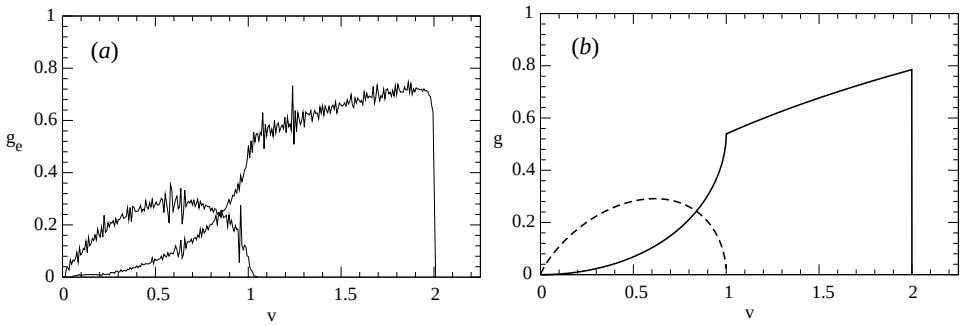

Figure 4. Distribution of crossings $g(v)$ according to the relative difference between the slopes v. (*a*) Exact quantum results. (*b*) Results predicted for the smooth part of the density of crossings. The dashed curve corresponds to crossings between levels with equal sign of their slopes, while the solid curve corresponds to crossings between levels with different sign.

with

$$g(v) = \begin{cases} g_I(v)^+ + g_I(v)^- & \text{if} \quad v \leqslant 1 \\ g_{II}(v)^- & \text{if} \quad 1 < v \leqslant 2. \end{cases} \tag{2.25}$$

As in the rectangular billiard, distribution equation (2.25) holds irrespective of the values of the flux and the energy. Therefore, the distribution of crossing below an energy ϵ according to the value of v will be given by

$$\left\langle \frac{\mathrm{d}n_c(\epsilon, \mu, v)}{\mathrm{d}v} \right\rangle = g(v) \int_0^{\epsilon} \langle \rho_c(\epsilon', \mu) \rangle \, \mathrm{d}\epsilon'$$
$$= \frac{4}{3} \frac{(\epsilon)^{3/2}}{\sqrt{\gamma}} g(v). \tag{2.26}$$

Figure 4 shows $g(v)$ predicted by equations (2.23) together with the exact quantum results obtained computing the crossings for $\epsilon < 1400$ between $0 \leqslant \mu < 1$ ($n_c = 105\,158$ crossings). We have discriminated the crossings according to whether the slopes of the levels have the same sign ($g_I(v)^+$, dashed curve) or different sign ($g_I^- + g_{II}^-$, solid curve). Note that there are $n_c^+ = 22\,266$ crossings (+) and $n_c^- = 82\,892$ crossings (−). These results are consistent with equation (2.19) which implies

$$\frac{n_c^+}{n_c} = 2 - \frac{\pi}{2}$$
$$\frac{n_c^-}{n_c} = \frac{\pi}{2}. \tag{2.27}$$

3. The oscillating contributions

In this section we calculate the oscillating contributions to the density of crossings, equation (1.25). They are determined by the periodic orbits that satisfy condition equation (1.23).

3.1. Rectangular billiards

Given the Hamiltonian equation (2.1) the periodic orbits are classified according to the topology (m_1, m_2), $m_1(m_2)$ being the number of bounces on a side of length $b(a)$ before the periodic orbits are closed.

Taking into account equation (2.1) and the requirement equation (1.23), we have

$$\frac{I_1^o \mu^2}{I_2^o} = \frac{m_1}{m_2} \tag{3.1}$$

and

$$\begin{aligned} I_1^o(m_1, m_2) &= \left(\frac{\epsilon}{\frac{m_1^2}{\mu} + m_2^2 \mu} \right)^{1/2} \frac{m_1}{\mu} \\ I_2^o(m_1, m_2) &= \left(\frac{\epsilon}{\frac{m_1^2}{\mu} + m_2^2 \mu} \right)^{1/2} m_2 \mu. \end{aligned} \tag{3.2}$$

Therefore, from equations (1.27) and (1.28) follows

$$S(m_1, m_2) = 2\pi \sqrt{\left(\frac{m_1^2}{\mu} + m_2^2 \mu \right) \epsilon} \tag{3.3}$$

$$\theta(m_1, m_2) = -\frac{\pi}{4}. \tag{3.4}$$

On the other hand, using equation (2.3), we have

$$\left| \frac{\mathrm{d}^2 I_2}{\mathrm{d} I_1^2} \right| = \frac{\mu^3 \epsilon}{I_2^3}. \tag{3.5}$$

We replace equations (3.2), (3.3) and (3.5) in equation (1.25), and performing elemental integrations we obtain the oscillating contributions

$$\begin{aligned} \rho_c(\epsilon, \mu)_{osc1} = \sum_{m_1, m_2 \neq (0,0)} & \left(\frac{\epsilon}{\mu} \right)^{3/4} \frac{1}{(m_1^2 + m_2^2 \mu^2)^{1/4}} \left[\frac{(4 m_1 m_2 \mu + \pi m_2^2 \mu^2 - \pi m_1^2)}{8(m_1^2 + m_2^2 \mu^2)} \right. \\ & \left. + \frac{(m_1^2 - m_2^2 \mu^2)}{2(m_1^2 + m_2^2 \mu^2)} \arcsin \left(\frac{m_1}{\sqrt{m_1^2 + m_2^2 \mu^2}} \right) \right] \\ & \times \cos \left(2\pi \sqrt{\left(\frac{m_1^2}{\mu} + m_2^2 \mu \right) \epsilon} - \frac{\pi}{4} \right). \end{aligned} \tag{3.6}$$

On the other hand, replacing equations (3.2), (3.3) and (3.5) in equation (1.30) we obtain

$$\begin{aligned} \rho_c(\epsilon, \mu)_{osc2} = \sum_{m_1, m_2 \neq (0,0)} \sum_{m_1', m_2' \neq (0,0)} & \left(\frac{\epsilon}{\mu} \right)^{1/2} \frac{1}{(m_1^2 + m_2^2 \mu^2)^{1/4} (m_1'^2 + m_2'^2 \mu^2)^{1/4}} \\ & \times \left| \frac{m_1^2}{(m_1^2 + m_2^2 \mu^2)} - \frac{m_1'^2}{(m_1'^2 + m_2'^2 \mu^2)} \right| \\ & \times \cos \left(2\pi \sqrt{\left(\frac{m_1^2}{\mu} + m_2^2 \mu \right) \epsilon} - \frac{\pi}{4} \right) \cos \left(2\pi \sqrt{\left(\frac{m_1'^2}{\mu} + m_2'^2 \mu \right) \epsilon} - \frac{\pi}{4} \right). \end{aligned} \tag{3.7}$$

Unlike the smooth part, equation (2.7), both contributions involve information about the individual crossings. The calculation of $\rho_c(\epsilon, \mu)_{osc2}$ implies a quadruple sum (over m_1, m_2, m_1', m_2') while $\rho_c(\epsilon, \mu)_{osc1}$ is a double sum. However, if we consider only $\rho_c(\epsilon, \mu)_{osc1}$ we have a satisfactory resolution of the individual crossings in the plane ϵ–μ as can be seen in figure 5. This figure shows a region in the plane ϵ–μ where there are three crossings. In figure 5(*a*) the exact quantum levels are plotted. Figure 5(*b*) shows the oscillating part, equation (1.25), considering m_1 and m_2 up to 150.

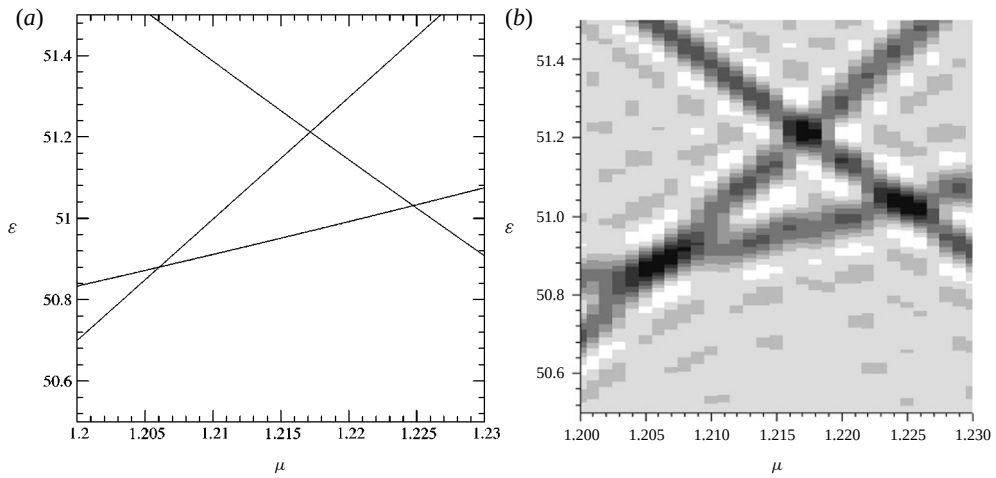

Figure 5. (*a*) Detail of three exact quantum eigenenergies for the rectangular billiard as a function of μ where three crossings can be observed. (*b*) Density plot of the oscillating part $\rho_{c_{osc1}}$ (see section 3.1 in the text) of the density of crossings in the same region of the plane ϵ–μ.

3.2. Aharonov–Bohm cylindrical billiards

In this example, the periodic orbits are labelled by the number of rotations around the axis of the cylinder (m_1) and the number of bounces on the base of the cylindrical surface (m_2) before the periodic orbits are closed. Taking into account that

$$\frac{I_1^o \gamma}{I_2^o} = \frac{m_1}{m_2} \tag{3.8}$$

and

$$\begin{aligned} I_1^o(m_1, m_2) &= \left(\frac{\epsilon}{\gamma(m_1^2 + \gamma m_2^2)}\right)^{1/2} m_1 \\ I_2^o(m_1, m_2) &= \left(\frac{\gamma\epsilon}{(m_1^2 + \gamma m_2^2)}\right)^{1/2} m_2 \\ S(m_1, m_2) &= 2\pi\sqrt{\frac{\epsilon}{\gamma}(m_1^2 + \gamma m_2^2)} \\ \frac{\mathrm{d}^2 I_2}{\mathrm{d}I_1^2} &= \frac{\gamma\epsilon}{I_2^3} \end{aligned} \tag{3.9}$$

we obtain (for details see the appendix):

$$\begin{aligned} \rho_c(\epsilon, \mu)_{osc1} = \sum_{m_1, m_2 \neq (0,0)} \Delta_{m_1} \left[\frac{\epsilon}{\gamma(m_1^2 + \gamma m_2^2)}\right]^{1/4} \left[\frac{m_1}{\sqrt{m_1^2 + \gamma m_2^2}} \arcsin\left(\frac{m_1}{\sqrt{m_1^2 + \gamma m_2^2}}\right)\right. \\ \left. + \frac{\sqrt{\gamma} m_2}{\sqrt{m_1^2 + \gamma m_2^2}}\right] \times \cos\left(2\pi\sqrt{\frac{\epsilon}{\gamma}(m_1^2 + \gamma m_2^2)} - \frac{\pi}{4}\right) \cos(2\pi m_1 \mu) \end{aligned} \tag{3.10}$$

where $\Delta_{m_1} = 2$ if $m_1 \neq 0$ and $\Delta_0 = 1$, and

$$\rho_c(\epsilon, \mu)_{osc2} = \sum_{m_1, m_2 \neq (0,0)} \sum_{m_1', m_2' \neq (0,0)} \left| \frac{m_1}{(m_1^2 + \gamma m_2^2)} - \frac{m_1'}{(m_1'^2 + \gamma m_2'^2)} \right|$$

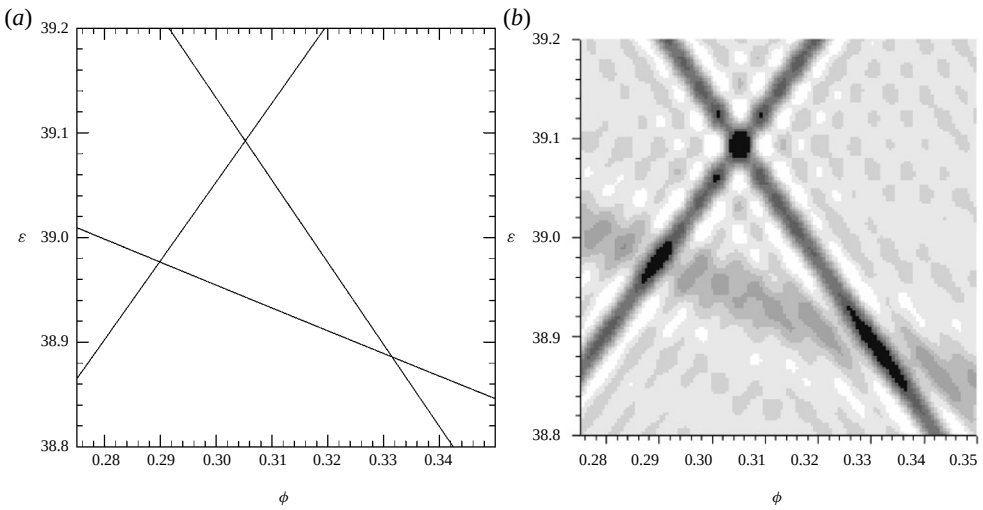

Figure 6. (*a*) Detail of three exact quantum eigenenergies for the Aharonov–Bohm cylindrical billiard as a function of the flux ϕ where three crossings can be observed. (*b*) Density plot of the oscillating part $\rho_{c_{osc1}}$ (see section 3.2 in the text) of the density of crossings in the same region of the plane ϵ–ϕ.

$$
\begin{aligned}
&\times\left[\cos\left(2\pi\left(\sqrt{\frac{\epsilon}{\gamma}(m_1^2+\gamma m_2^2)}-\sqrt{\frac{\epsilon}{\gamma}(m_1'^2+\gamma m_2'^2)}\right)\right)\right.\\
&\times\cos\left(2\pi(m_1-m_1')\mu\right)\\
&+\cos\left(2\pi\left(\sqrt{\frac{\epsilon}{\gamma}(m_1^2+\gamma m_2^2)}+\sqrt{\frac{\epsilon}{\gamma}(m_1'^2+\gamma m_2'^2)}-\frac{1}{4}\right)\right)\\
&\left.\times\cos\left(2\pi(m_1+m_1')\mu\right)\right]\\
&+\left[\frac{m_1}{(m_1^2+\gamma m_2^2)}+\frac{m_1'}{(m_1'^2+\gamma m_2'^2)}\right]\\
&\times\left[\cos\left(2\pi\left(\sqrt{\frac{\epsilon}{\gamma}(m_1^2+\gamma m_2^2)}+\sqrt{\frac{\epsilon}{\gamma}(m_1'^2+\gamma m_2'^2)}-\frac{1}{4}\right)\right)\right.\\
&\times\cos\left(2\pi(m_1-m_1')\mu\right)\\
&\left.+\cos\left(2\pi\left(\sqrt{\frac{\epsilon}{\gamma}(m_1^2+\gamma m_2^2)}-\sqrt{\frac{\epsilon}{\gamma}(m_1'^2+\gamma m_2'^2)}\right)\right)\cos\left(2\pi(m_1+m_1')\mu\right)\right].
\end{aligned}
\tag{3.11}
$$

As in the example of the previous section, $\rho_c(\epsilon,\mu)_{osc1}$ (equation (3.10)) gives enough information to determine individual crossings, as can be seen in figure 6. In figure 6(*a*) is depicted a region of the plane ϵ–μ where the exact quantum levels show three crossings. Figure 6(*b*) shows the oscillating contribution given by equation (3.10) taking into account m_1 and m_2 up to 150.

Unlike the rectangular billiard, in the present case the dependence on the parameter μ of the oscillating contributions is quite simple. Therefore, equations (3.10) and (3.11) can be easily integrated to obtain the oscillating part of the number of crossings in the energy interval

$[\epsilon, \epsilon + \mathrm{d}\epsilon]$ per unity of flux,

$$\frac{\mathrm{d}n_c}{\mathrm{d}\epsilon} = \int_{\mu=0}^{\mu=1} \rho_c(\epsilon, \mu)\,\mathrm{d}\mu = \int_{\mu=0}^{\mu=1} \langle\rho_c\rangle\,\mathrm{d}\mu + \int_{\mu=0}^{\mu=1} \rho_c(\epsilon, \mu)_{osc1}\,\mathrm{d}\mu + \int_{\mu=0}^{\mu=1} \rho_c(\epsilon, \mu)_{osc2}\,\mathrm{d}\mu. \quad (3.12)$$

As we pointed out in section 2, the smooth part of the density of crossings depends only on the energy ϵ, so the integrated smooth part (the first integral in the right-hand side of equation (3.12)) is given by equation (2.18). For the oscillating contributions, the integration over μ of the terms in equation (3.10) vanishes unless $m_1 = 0$ (because they are proportional to $\sin(2\pi m_1)/2\pi m_1$). Therefore, we obtain

$$\int_{\mu=0}^{\mu=1} \rho_c(\epsilon, \mu)_{osc1}\,\mathrm{d}\mu = 2\left(\frac{\epsilon}{\gamma}\right)^{\frac{1}{4}} \sum_{m_2>0} \frac{1}{m_2^{\frac{1}{2}}} \cos\left(2\pi m_2\sqrt{\epsilon} - \frac{\pi}{4}\right). \quad (3.13)$$

In terms of the classical motion, the contribution equation (3.13) is originated by the orbits that, having $m_1 = 0$, correspond to an irrotational motion with bounces between the bases of the cylinder. Figure 7(*a*) shows the exact quantum calculation of the integrated density of crossings obtained through a histogram. The sum of the contribution equation (3.13) (up to $m_2 = 500$) and the smooth part, equation (2.18), is shown in figure 7(*b*). We can see that the contribution of the oscillating term (3.13) originates the sharp peaks that are present in the exact calculation. By inspection of (3.13), we expect a sharp peak whenever ϵ approaches a value such that

$$m_2\sqrt{\epsilon} - \tfrac{1}{8} = l \quad (3.14)$$

for all m_2 with l being an integer. For $\epsilon \gg 1$ this condition leads to $\epsilon \approx n^2$. Therefore we conclude that the peaks correspond to the regions of energy where a 'head-rotational band' state appears. Such states (the first state for a given n) are the least affected by a change of the flux (μ) (they have the smallest slope because they have angular momentum equal to zero) and they contribute to the density of crossings in a relevant way because they will cross with all the other states that go through (upward or downward) this region of energy. The integration of the terms corresponding to the other oscillating contribution (3.11) also vanishes unless $m_1 = m_1'$. Taking into account these contributions, the integrated density of crossings is shown in figure 7(*c*).

4. Concluding remarks

In this paper we have derived a semiclassical expression for the density of degeneracies, $\rho_c(E, \mu)$, that occur in quantum integrable systems depending on a single parameter μ. We have applied our results to two specific systems that depend on the parameter in a different functional form, obtaining a quite satisfactory agreement with the exact quantum calculation. Our results show that the density of crossings is strongly dependent on the derivative of the Hamiltonian with respect to the parameter. Therefore, unlike the density of states, even the smooth part of the density of crossings can depend on the energy E and on the parameter μ in a diverse way according to the functional form of $H(\mu)$. In particular, the smooth part of ρ_c for the rectangular billiard, where μ is the ratio between its sides, is $\sim E/\mu$. Taking into account that the origin of the crossings between eigenenergies of integrable billiards as a function of a shape parameter has the same and very simple interpretation in terms of geometrical arguments [13], we expect that the dependence $\sim E/\mu$ of the smooth part of the density of

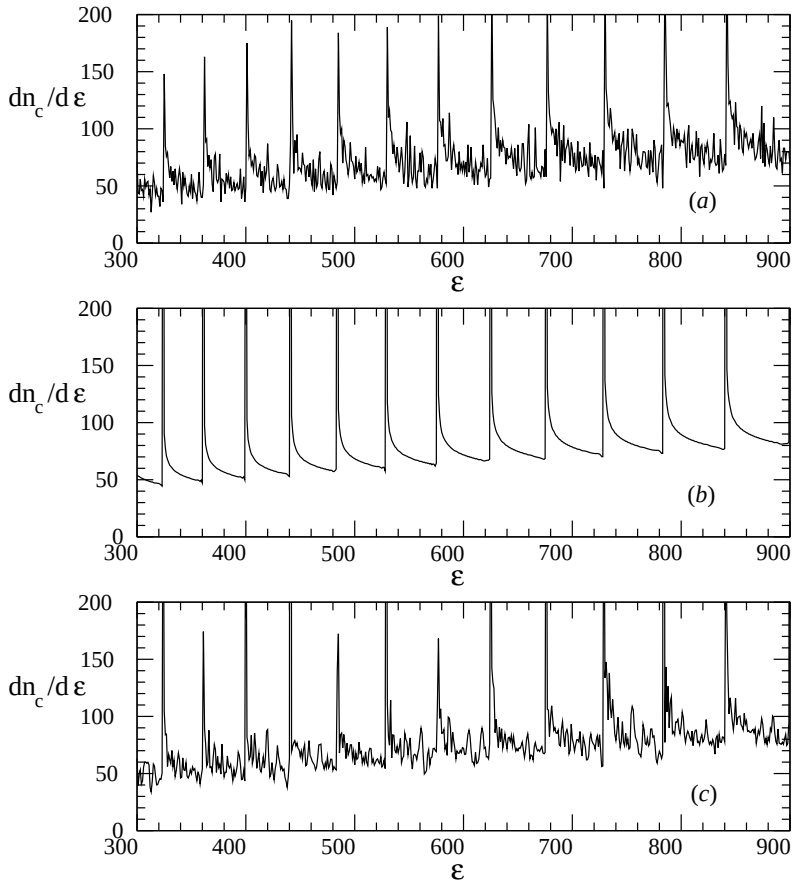

Figure 7. (*a*) Integrated density of crossings $\frac{dn_c}{d\epsilon}$ as a function of energy ϵ for the Aharonov–Bohm cylindrical billiard with $\gamma = \frac{4}{\pi^2}$. (*b*) The same density predicted by the sum of the smooth part $\langle\rho_c\rangle$ and the contribution originated by $\rho_{c_{osc1}}$. (*c*) The same density predicted by $\langle\rho_c\rangle + \rho_{c_{osc1}} + \rho_{c_{osc2}}$ (see section 3.2 in the text).

crossings holds for any integrable billiard (like the elliptic billiard where μ is the ratio between the axes of the elliptical box or the annular billiard where μ is the ratio between the outer and inner radii). On the other hand, for the Bunimovich stadium [14], there are numerical evidences that the smooth part of the integrated density of narrowly avoided crossings (that is the number of narrowly avoided crossings per unit of E for a given interval of μ, being μ the shape parameter), shows a linear dependence on the energy E. This suggests that the integrated distribution of narrowly avoided crossings when μ is a shape parameter would have the same functional dependence on E (linear) for other irregular billiards.

For the Aharonov–Bohm cylindrical billiard, the smooth part of the density of crossings is $\sim\sqrt{E}$ without dependence on $\mu = \phi$ (the magnetic flux). Such a result can be understood using very simple semiclassical arguments. Let us consider the Fermi surface (for the two-dimensional systems Fermi curve) defined by $H(n_1, n_2, \phi = 0) = E$ in the plane (n_1, n_2). The number of states below the energy E is proportional to the area enclosed by the Fermi curve, that is proportional to E. When ϕ varies in one fluxoid, the Fermi curve is rigidly translated in the plane (n_1, n_2) defining a new curve $H(n_1, n_2, \phi = 1) = E$. The number of crossings

(between $\phi = 0$ and $\phi = 1$) is proportional to the number of points that lie in the thin shell defined by these two curves. This number scales as the length of the Fermi curve, that is $\propto\sqrt{E}$. Such functional form should hold for other Aharonov–Bohm integrable billiards and this is the case for the Aharonov–Bohm annular billiard [15]. Moreover, in [15] it is shown, by numerical computation, that the distribution of spacing in flux between crossings that a given level has, is Poissonian. This paper provides the framework to study properties of the crossing spacing distribution, employing the two-point correlation function for the density of degeneracies.

Appendix A

In this appendix we discuss the contribution of the diagonal terms in equation (1.6) to the semiclassical density of degeneracies. These terms, where $\vec{n} = \vec{n'}$, correspond to 'self-crossings'. It is evident that they are not genuine degeneracies and, at first glance, we should subtract them from equation (1.6). However, as we will show below, these contributions vanish in the semiclassical limit. In fact, when $\vec{n} = \vec{n'}$, equation (1.11) that defines the values of μ for which there is a degeneracy, is fulfilled for all μ. In such a case

$$\rho_c^d \equiv \tfrac{1}{2}\sum_{\vec{n}} \delta(E - H(\vec{n}, \mu)) = \tfrac{1}{2}\rho_s. \tag{A1}$$

Therefore ρ_c^d, the diagonal contribution of ρ_c, is equal to one-half of the density of states ρ_s. For simplicity, in (A1) we adimensionalize μ appropriately. Following [2], the semiclassical density of states for a system having k degrees of freedom can be written as

$$\rho_s = \langle\rho_s\rangle + \rho_{osc} \tag{A2}$$

where $\langle\rho_s\rangle \sim \frac{1}{\hbar^k}$ and $\rho_{osc} \sim \frac{1}{\hbar^{(k+1)/2}}$. Moreover, as we have shown in this paper, in the semiclassical limit, equation (1.6) is

$$\rho_c = \langle\rho_c\rangle + \rho_{osc1} + \rho_{osc2} \tag{A3}$$

where $\langle\rho_c\rangle \sim \frac{1}{\hbar^{2k}}$, $\rho_{osc1} \sim \frac{1}{\hbar^{(3k+1)/2}}$ and $\rho_{osc2} \sim \frac{1}{\hbar^{(k+1)}}$. Therefore, in the semiclassical limit we neglect terms ρ_{c_i} such that $\rho_{c_i} \sim \frac{1}{\hbar^\beta}$ with $\beta < (k+1)$. In particular, as the diagonal contribution (A1) is $\sim \frac{1}{\hbar^k}$, it does not contribute to the semiclassical density of degeneracies and it is not necessary to subtract it from equation (1.6). On the other hand, in the calculations performed in this paper for billiards, we have set $\hbar = 1$ and the semiclassical limit corresponds to high-energy states. For low energies subtraction of the self-crossings would be necessary. By inspection of figure 1 this seems to be the case. There we have plotted the smooth part of the integrated density of crossings, equation (2.7), without the corrections for the self-crossings. This could explain the fact that the theoretical curves are somewhat above the numerical ones in figure 1.

Appendix B

This appendix is devoted to showing how to handle the sum equation (1.6) for the Aharonov–Bohm cylindrical billiard. For this system, having one degree of freedom of rotation, the conjugated states by time reversal transformation are not degenerated.

First, let us consider the billiard without flux. The eigenenergies are

$$h(n_1, n_2) = \gamma n_1^2 + (n_2 + 1)^2 \tag{B1}$$

where n_1 is the quantum number related to the rotation around the axis of the cylinder ($n_1 = 0, \pm1, \pm2, \ldots$) and n_2 is the quantum number related to libration motion parallel to the

axis ($n_2 = 0, 1, 2, 3$). The system has Kramers'000000 degeneracy. A quantum eigenstate (n_1, n_2) and its conjugate $(-n_1, n_2)$ have the same eigenenergy if $n_1 \neq 0$. To take into account these degeneracies in the sum equation (1.6) over $n_1, n_1' \geqslant 0$ we must include a factor $e(n_1, n_1')$ in each term such that

$$e(n_1, n_1') = \begin{cases} 4 & \text{if} \quad n_1 \neq 0 \quad \text{and} \quad n_1' \neq 0 \\ 2 & \text{if} \quad (n_1 \neq 0 \quad \text{and} \quad n_1' = 0) \quad \text{or} \quad (n_1 \neq 0 \quad \text{and} \quad n_1' \neq 0) \\ 0 & \text{if} \quad n_1 = 0 \quad \text{and} \quad n_1' = 0. \end{cases} \tag{B2}$$

When the cylinder is threaded by a magnetic flux ϕ, the eigenenergies of a conjugate pairs of eigenstates are

$$\begin{aligned} h(n_1, n_2, \phi) &= \gamma(n_1 - \phi)^2 + (n_2 + 1)^2 \\ h(-n_1, n_2, \phi) &= \gamma(-n_1 - \phi)^2 + (n_2 + 1)^2 = \gamma(n_1 + \phi)^2 + (n_2 + 1)^2. \end{aligned} \tag{B3}$$

Therefore, conjugated pairs of eigenstates are no longer degenerated. In such a situation, to preserve the sum equation (1.6) over $n_1, n_1' \geqslant 0$, we must distinguish two kinds of states according to the dependence on the flux that their eigenenergies have. Moreover, equation (1.5) which determines the values of the parameter for which the crossings occur, changes according to the same dependence. Thus, equation (1.6) for the cylindrical billiard means

$$\begin{aligned} \rho_c(\epsilon, \phi) = {} & \tfrac{1}{2} \sum_{\vec{n}} \sum_{\vec{n}'} \delta(\epsilon - h(n_1 + \phi, n_2))\delta(\phi - L_1(n_1, n_2, n_1', n_2')) \\ & + \tfrac{1}{2} \sum_{\vec{n} \neq (0, n_2)} \sum_{\vec{n}' \neq (0, n_2')} \delta(\epsilon - h(n_1 - \phi, n_2))\delta(\phi - L_2(n_1, n_2, n_1', n_2')) \\ & + \tfrac{1}{2} \sum_{\vec{n}} \sum_{\vec{n}' \neq (0, n_2')} \delta(\epsilon - h(n_1 - \phi, n_2))\delta(\phi - L_3(n_1, n_2, n_1', n_2')) \\ & + \tfrac{1}{2} \sum_{\vec{n} \neq (0, n_2)} \sum_{\vec{n}'} \delta(\epsilon - h(n_1 + \phi, n_2))\delta(\phi - L_3(n_1, n_2, n_1', n_2')) \end{aligned} \tag{B4}$$

where L_1, L_2 and L_3 are the values of the flux determined by the roots of

$$\begin{aligned} & h(n_1 + \phi, n_2) - h(n_1' + \phi, n_2') = 0 \\ & h(n_1 - \phi, n_2) - h(n_1' - \phi, n_2') = 0 \\ & h(n_1 - \phi, n_2) - h(n_1' + \phi, n_2') = 0 \end{aligned} \tag{B5}$$

respectively.

Now we employ Poisson's formula. The first sum in equation (B4), which takes into account the crossings between energy levels that increase as a function of ϕ (this term includes the crossings between levels $(n_1 = 0, n_2)$ and $(n_1' = 0, n_2)$), can be written as

$$\begin{aligned} & \tfrac{1}{2} \sum_{m_1, m_2} \sum_{m_1', m_2'} \int_{\vec{I} \geqslant (0,0)} \int_{\vec{I}' \geqslant (0,0)} \delta(\epsilon - h(I_1 + \phi, I_2))\delta(\phi - L(I_1 + \phi, I_2, I_1' + \phi, I_2') \\ & \qquad \times \exp(\mathrm{i}2\pi(\vec{m} \cdot \vec{I} + \vec{m}' \cdot \vec{I}')) \end{aligned} \tag{B6}$$

where we have taken into account that $\alpha_1 = 0$ and $\alpha_2 = 4$. To eliminate the δ functions we employ equations (1.7)–(1.18) together with the first equation of (B5). We obtain

$$\begin{aligned} \rho_c(\epsilon, \phi, +, +) = {} & \frac{\gamma}{2} \sum_{\vec{m}} \sum_{\vec{m}'} \int_{I_1 \geqslant 0} \int_{I_1' \geqslant 0} \mathrm{d}I_1 \, \mathrm{d}I_1' \frac{|I_1 - I_1'|}{2\sqrt{\epsilon - \gamma(I_1 + \phi)^2}\sqrt{\epsilon - \gamma(I_1' + \phi)^2}} \\ & \times \exp(\mathrm{i}2\pi(m_1 I_1 + m_2 I_2 + m_1' I_1' + m_2' I_2')). \end{aligned} \tag{B7}$$

Now, we redefine $\bar{I}_1(\bar{I}_1') \equiv I_1 + \phi(I_1' + \phi)$. After replacing it, we have

$$\rho_c(\epsilon,\phi,+,+) = \frac{\gamma}{2}\sum_{\vec{m}}\sum_{\vec{m}'}\int_{I_1\geqslant\phi}\int_{I_1'\geqslant\phi} \mathrm{d}I_1\,\mathrm{d}I_1' \frac{|I_1 - I_1'|}{2\sqrt{\epsilon-\gamma I_1^2}\sqrt{\epsilon-\gamma I_1^{2\prime}}} \times \exp\left(\mathrm{i}2\pi(m_1(I_1-\phi) + m_2 I_2 + m_1'(I_1'-\phi) + m_2' I_2')\right) \tag{B8}$$

where we have omitted the bar in the integration variables. In the same way, the second sum in (B4) (using the second equation of (B5)) and the third and fourth (using the third equation of (B5)) are

$$\rho_c(\epsilon,\phi,-,-) = \frac{\gamma}{2}\sum_{\vec{m}}\sum_{\vec{m}'}\int_{I_1\geqslant-\phi}\int_{I_1'\geqslant-\phi} \mathrm{d}I_1\,\mathrm{d}I_1' \frac{|I_1 - I_1'|}{2\sqrt{\epsilon-\gamma I_1^2}\sqrt{\epsilon-\gamma I_1^{2\prime}}} \times \exp\left(\mathrm{i}2\pi(m_1(I_1+\phi) + m_2 I_2 + m_1'(I_1'+\phi) + m_2' I_2')\right) \tag{B9}$$

$$\rho_c(\epsilon,\phi,+,-) = \frac{\gamma}{2}\sum_{\vec{m}}\sum_{\vec{m}'}\int_{I_1\geqslant\phi}\int_{I_1'\geqslant-\phi} \mathrm{d}I_1\,\mathrm{d}I_1' \frac{(I_1 + I_1')}{2\sqrt{\epsilon-\gamma I_1^2}\sqrt{\epsilon-\gamma I_1^{2\prime}}} \times \exp\left(\mathrm{i}2\pi(m_1(I_1-\phi) + m_2 I_2 + m_1'(I_1'+\phi) + m_2' I_2')\right) \tag{B10}$$

$$\rho_c(\epsilon,\phi,-,+) = \frac{\gamma}{2}\sum_{\vec{m}}\sum_{\vec{m}'}\int_{I_1\geqslant-\phi}\int_{I_1'\geqslant\phi} \mathrm{d}I_1\,\mathrm{d}I_1' \frac{(I_1 + I_1')}{2\sqrt{\epsilon-\gamma I_1^2}\sqrt{\epsilon-\gamma I_1^{2\prime}}} \times \exp\left(\mathrm{i}2\pi(m_1(I_1+\phi) + m_2 I_2 + m_1'(I_1'-\phi) + m_2' I_2')\right). \tag{B11}$$

Equation (B9) takes into account the crossings between energy levels that decrease as a function of ϕ while equations (B10) and (B11) correspond to crossings between levels that increase and decrease as a function of ϕ. For the smooth part, we set $m_1 = m_2 = m_1' = m_2' = 0$ in the sum of equations (B8)–(B11) and taking into account that the lower limit in the integration over I_i can be taken as 0 (because $\epsilon \gg 1$ implies $\phi \to 0^+$ and $-\phi \to 0^-$) we obtain equation (2.17).

To obtain the first contribution to the oscillating part $\rho_c(\epsilon,\phi)_{osc1}$, equation (1.25), we set $m_1 = m_2 = 0$ and we integrate over I_1. Then, we approximate the integration over I_1' using the stationary phase technique, obtaining equation (3.10). For the second contribution, $\rho_c(\epsilon,\phi)_{osc2}$, we evaluate both integrals (over I_1 and I_2) in the stationary phase condition. The resulting equation (3.11) is long but straightforward. However, we will mention some steps. After replacing the stationary phase condition for the actions and reducing the sums over m_i and m_i' to the positive quadrants we have in equations (B8) and (B9) terms like (we write the prefactors as A),

$$\begin{aligned} &2A\cos(S - 2\pi m_1\phi) - \frac{\pi}{4}\cos\left(S' - 2\pi m_1'\phi - \frac{\pi}{4}\right) \\ &2A\cos(S + 2\pi m_1\phi) - \frac{\pi}{4}\cos\left(S' + 2\pi m_1'\phi - \frac{\pi}{4}\right) \end{aligned} \tag{B12}$$

respectively. These terms can be appropriately combined using trigonometric identities in the form

$$A[\cos(S-S')\cos(2\pi\phi(m_1 - m_1')) + \cos(S+S'+\pi/2)\cos(2\pi\phi(m_1+m_1'))]. \tag{B13}$$

In the same way the terms of equations (B10) and (B11) result:

$$\begin{aligned} &2B\cos\left(S - 2\pi m_1\phi - \frac{\pi}{4}\right)\cos\left(S' + 2\pi m_1'\phi - \frac{\pi}{4}\right) \\ &2B\cos\left(S + 2\pi m_1\phi - \frac{\pi}{4}\right)\cos\left(S' - 2\pi m_1'\phi - \frac{\pi}{4}\right). \end{aligned} \tag{B14}$$

Therefore, the sum of these terms is

$$B[\cos(S-S')\cos(2\pi\phi(m_1 + m_1')) + \cos(S+S'+\pi/2)\cos(2\pi\phi(m_1-m_1'))] \tag{B15}$$

and equation (3.11) follows. Note that equations (B12) and (B14) are a consequence of the breaking of the time reversal symmetry when the magnetic flux is present. In such a case, twin classical orbits (related to each other by the time reversal transformation) that have the same action when the systems has the time reversal symmetry split their actions when the flux is applied [16].

Acknowledgments

This work was partially supported by UBACYT (TW35), PICT97 03-00050-01015 and CONICET.

References

[1] Percival I C 1973 *J. Phys. B: At. Mol. Phys.* **6** L229
[2] Berry M V and Tabor M 1977 *Proc. R. Soc.* A **356** 375
[3] Pechucas T 1983 *Phys. Rev. Lett.* **51** 943
[4] Bohigas A, Giannoni M J and Schmit C 1984 *J. Phys. Lett.* **45** L1015
[5] Yukawa T 1985 *Phys. Rev. Lett.* **54** 1883
[6] Berry M V and Wilkinson M 1984 *Proc. R. Soc.* A **392** 45
[7] Wilkinson M 1988 *J. Phys. A: Math. Gen.* **21** 1173
[8] Wilkinson M 1989 *J. Phys. A: Math. Gen.* **22** 2795
[9] Wilkinson M and Austin E J 1993 *Phys. Rev.* A **47** 2601
[10] Walker P, Sánchez M J and Wilkinson M 1996 *J. Math. Phys.* **37** 5019
[11] Berry M V and Tabor M 1976 *Proc. R. Soc.* A **349** 101
[12] Gutzwiller M C 1990 *Chaos in Classical and Quantum Mechanics* (New York: Springer)
[13] Traiber A J S, Fendrik A J and Bernath M 1989 *J. Phys. A: Math. Gen.* **22** L365
[14] Sánchez M J, Vergini E and Wisniacki D 1996 *Phys. Rev.* E **54** 4812
[15] Fendrik A J and Sánchez M J 2000 *Eur. Phys. J.* B at press
(Fendrik A J and Sánchez M J 1998 *Preprint* cond-mat/9811272)
[16] Bohigas O, Giannoni M J, Ozorio de Almeida A M and Schmit C 1995 *Nonlinearity* **8** 203